Available online at www.sciencedirect.com
ScienceDirect
Biochimica et Biophysica Acta 1768 (2007) 439–449
Biochimica et Biophysica Acta
BBA
www.elsevier.com/locate/bbamem

Profilin binding to sub-micellar concentrations of phosphatidylinositol (4,5) bisphosphate and phosphatidylinositol (3,4,5) trisphosphate

Pierre D.J. Moens [a,*], Luis A. Bagatolli [b]

[a] School of Biological, Biomedical and Molecular Sciences, The University of New England, Armidale, NSW 2351 Australia
[b] MEMPHYS-Center for Biomembrane Physics, Department of Biochemistry and Molecular Biology, University of Southern Denmark Campusvej 55, DK-5230 Odense M, Denmark

Received 6 July 2006; received in revised form 20 November 2006; accepted 14 December 2006
Available online 23 December 2006

Abstract

Profilin is a small (12–15 kDa) actin binding protein which promotes filament turnover. Profilin is also involved in the signaling pathway linking receptors in the cell membrane to the microfilament system within the cell. Profilin is thought to play critical roles in this signaling pathway through its interaction with phosphatidylinositol 4,5-bisphosphate [PI(4,5)P_2] and phosphatidylinositol 3,4,5-trisphosphate [PI(3,4,5)P_3] (P.J. Lu, W.R. Shieh, S.G. Rhee, H.L. Yin, C.S. Chen, Lipid products of phosphoinositide 3-kinase bind human profilin with high affinity, Biochemistry 35 (1996) 14027–14034). To date, profilin's interaction with polyphosphoinositides (PPI) has only been studied in micelles or small vesicles. Profilin binds with high affinity to small clusters of PI(4,5)P_2 molecules. In this work, we investigated the interactions of profilin with sub-micellar concentrations of PI(4,5)P_2 and PI(3,4,5)P_3. Fluorescence anisotropy was used to determine the relevant dissociation constants for binding of sub-micellar concentrations of fluorescently labeled PPI lipids to profilin and we show that these are significantly different from those determined for profilin interaction with micelles or small vesicles. We also show that profilin binds more tightly to sub-micellar concentrations of PI(3,4,5)P_3 (K_D=720 μM) than to sub-micellar concentrations of PI(4,5)P_2 (K_D=985 μM). Despite the low affinity for sub-micellar concentration of PI(4,5)P_2, profilin was shown to bind to giant unilamellar vesicles in presence of 0.5% mole fraction of PI(4,5)P_2 The implications of these findings are discussed.

Keywords: Fluorescence spectroscopy; Anisotropy; Lifetime; FRET; PIP; GUV

1. Introduction

Profilin, a small ubiquitous non-muscle protein of 12–15 kDa, is found in eukaryotic cells [1,2], plants [3] and viruses [4]. Although profilin has been intensively studied since its discovery more than 20 years ago, its *in vivo* function is still poorly understood. In 1994, Haugwitz et al. [5] demonstrated that profilin is essential for the normal development and cytokinesis of *Dictyostelium amoeba*. They showed that in a profilin null mutant the motility of cells was significantly reduced and that the development was blocked prior to fruiting body formation. Furthermore, these cells could not be grown in shaking culture under normal conditions [5]. Profilin 1 is also essential for cell survival and cell division in mice [6]. Witke et al. showed that homozygous profilin null mutant (pfn1$^{ko/ko}$) mice are not viable [6]. Indeed, pfn1$^{ko/ko}$ embryos died as early as the two-cell stage and no pfn1$^{ko/ko}$ blastocysts were detectable.

The binding of profilin to actin monomers is probably one of the functions that have received the most attention in the last decade. Profilin binds actin monomers with a dissociation constant of 0.35–5 μM [7,8]. Together with cofilin, profilin promotes filament turnover. Profilin catalyses the exchange of nucleotides (ADP for ATP) in the actin cleft and prevents hydrolysis of bound ATP [8–10]. Profilin can facilitate actin polymerization by transporting monomers to the fast growing ends of filaments. However, in the current model of filamentous

Abbreviations: PI(4,5)P_2, phosphatidylinositol 4,5-bisphosphate; PI(3,4,5)P_3, phosphatidylinositol 3,4,5-trisphosphate; PPI, polyphosphoinositides; GUV, giant unilamellar vesicles

* Corresponding author. Tel.: +61 2 6773 3740; fax: +61 2 6773 3267.
E-mail address: pmoens@une.edu.au (P.D.J. Moens).

0005-2736/$ - see front matter © 2006 Elsevier B.V. All rights reserved.
doi:10.1016/j.bbamem.2006.12.012

actin, profilin and actin compete for the same binding site. Therefore, to add monomers to the growing end of the filament, profilin must either move to a new site on actin or completely dissociate (reviewed in [11]).

In *Saccharomyces cerevisiae*, profilin partitions between the plasma membrane and the cytosol in response to membrane phosphatidylinositol 4,5-bisphosphate [$PI(4,5)P_2$] levels. At rest, 80% of the profilin is associated with membrane phospholipids [12]. In resting platelets, Hartwig et al. [13] showed that 36% of the cell profilin is associated with the cell membrane. Upon activation by thrombin, these authors noted an increase of the fraction of profilin associated with the membrane to between 41 and 52%. Due to the interaction of profilin with $PI(4,5)P_2$ and phosphatidylinositol 3,4,5-trisphosphate [$PI(3,4,5)P_3$], profilin is thought to play critical roles in signaling pathways between the cell membrane and the cytoskeleton [14,15]. It is also well known that $PI(4,5)P_2$ micelles dissociates profilin from actin [16] and that profilin isolated from platelets binds with high affinity to small clusters of $PI(4,5)P_2$ molecules [17].

Profilin's binding to $PI(4,5)P_2$ micelles or small vesicles was studied using gel filtration [7,12,15,17], micro filtration [7], centrifugation [12] and fluorescence intensity measurements [15,18]. However, the dissociation constants reported vary by >200-fold (0.13 μM [12] to 35 μM [15]).

The exact binding region on profilin for polyphosphoinositides (PPI) is still not known. In 2002, Lambrechts et al. [7] and Skare and Karlsson [19] suggested the presence of two binding regions for $PI(4,5)P_2$ on human and mammalian profilin 1. One binding region is close to the binding site of poly (L-proline) and spans residues 126–136. The other includes residue 88 and overlaps with the actin-binding surface. Therefore, binding of PPI to the region spanning residues 126–136 allows for the formation of a ternary complex of actin:profilin:PPI, while binding of PPI to the region including residue 88 results in the dissociation of the profilin:actin complex.

The binding stoichiometry of $PI(4,5)P_2$ to profilin ranges from 5:1 in large unilamellar vesicles produced by the extrusion technique (LUVET), to 10:1 in micelles [14,15]. Goldschmidt-Clermont et al. suggested that this difference in binding stoichiometry could be due to steric hindrance among profilin molecules binding to micelles. This steric hindrance would result in an overestimation of the number of $PI(4,5)P_2$ molecules bound per profilin. They also suggested that profilin aggregates $PI(4,5)P_2$ into small patches [17].

The organization of $PI(4,5)P_2$ in cell membrane is clearly different from the organization of $PI(4,5)P_2$ in micelles and therefore, the binding of profilin to the membrane $PI(4,5)P_2$ could be different. It is possible that the initial binding of profilin starts with a single molecule of $PI(4,5)P_2$ which could be followed by a recruitment of additional $PI(4,5)P_2$ molecules by profilin forming small aggregates of $PI(4,5)P_2$ lipids. Alternatively, the initial binding of profilin to the membrane $PI(4,5)P_2$ could require the presence of small clusters of $PI(4,5)P_2$ lipids. In this paper, we investigate this question by studying the interaction of profilin with sub-micellar concentrations of PPI lipids and show that the binding of profilin to sub-micellar concentration of PPI is significantly weaker than the binding of profilin to $PI(4,5)P_2$ in micellar form or LUVET. However, we also observed binding of profilin to Giant unilamellar vesicles (GUV) containing only 0.5% of $PI(4,5)P_2$. Our FRET data suggest that the binding of profilin to the GUV recruits neighboring $PI(4,5)P_2$ molecules, stabilizing its interaction with the lipid membrane. We also show that the K_D of profilin for mono-dispersed $PI(3,4,5)P_3$ is lower than the K_D for mono-dispersed $PI(4,5)P_2$ [15].

2. Materials and methods

2.1. Polyphosphatidylinositols and lipids

Labeled PPI, i.e. BODIPY® TMR $PI(4,5)P_2$, BODIPY® TMR $PI(3,4,5)P_3$, BODIPY® FL $PI(4,5)P_2$, were purchased from Molecular Probes, Inc (Eugene, OR) or Echelon Biosciences, Inc (Salt Lake City, UT). Unlabeled L-α-Phosphatidylinositol-4,5-bisphosphate (Brain, Porcine-Triammonium Salt) and 1-palmitoyl 2-oleoyl-phosphatidylcholine (POPC) were purchased from Avanti Lipids, Inc (Alabaster, AL).

Homogeneous micelles of unlabeled $PI(4,5)P_2$ were prepared according to the procedure described by Goldschmidt-Clermont et al. [17]. Briefly, 1 mg of $PI(4,5)P_2$ per ml of MilliQ water was sonicated for 5 min at room temperature in a Bransonic Ultrasonic cleaner Model 2200.

2.2. Profilin cloning and purification

Profilin was purified from outdated human platelets as described in Janmey [20]. Human profilin 1 cDNA (MGC Clone ID: 3896948) was purchased from Invitrogen (Carlsbad, CA). Profilin cDNA was cut from the pCMV SPORT 6 vector using the restriction endonucleases *Nco*I and *Xho*I and was cloned into a pETBlue-2 vector (Novagen). The pETBlue-2 vector containing the profilin cDNA was transformed into the Rosetta 2(DE3)pLacI bacterial strain (Novagen) for expression and purification. Cells were lysed using 5 ml/g of wet cells of BugBuster HT reagent (Novagen). The cell lysate was then loaded on a poly-L proline affinity column and profilin was eluted using the same procedure as the one used for profilin isolated from human platelets. The purified profilin was renatured by extensive dialysis in 50 mM Tris buffer pH 7.

2.3. Spectroscopy

Light scattering, steady state anisotropy, Förster resonance energy transfer (FRET) and fluorescence lifetime measurements were carried out on an ISS K2 multifrequency phase and modulation spectrofluorometer (ISS, Inc., Champaign, IL) equipped with a 300 W Xenon arc lamp. Dynamic light scattering measurements were obtained on a Brookhaven PCS with a BI9000 correlator. The light source was a Spectra Physics 35 mW He/Ne laser at 632.8 nm.

2.3.1. Light scattering

The intensity of scattered light from 1 μM to 1 mM solutions of $PI(4,5)P_2$ was measured in a 4×10 mm cuvette using an excitation wavelength of 330 nm or 350 nm and looking at the light scattered at a 90° angle at the same wavelength as the excitation—the cuvettes were oriented with the shortpath towards the excitation source. During the measurements the intensity was corrected for the fluctuation of the exciting light using Rhodamine B in ethanol as a quantum counter. The average excitation counts obtained during the measurement was then used to normalize the scattering intensity between different samples and therefore compensate for changes in the excitation light between measurements. The intensity obtained was then corrected for the dilution of the $PI(4,5)P_2$ in each of the samples.

2.3.2. Fluorescence anisotropy

Excitation of the BODIPY® TMR PPI was at 540 nm and excitation of the BODIPY® FL $PI(4,5)P_2$ was at 505 nm. Fluorescence emission was recorded at wavelengths greater than 570 nm, observed through a Melles Griot Schott glass

type OG570 cut-off filter. The excitation bandwidth was set to 4 nm. Subtractions of blank samples containing the same concentration of profilin as the PPI samples were performed for each measurement. In each sample, the labeled PPI concentration was kept constant at 1 μM. The anisotropy of the sample was recorded at a controlled temperature of 20±0.1 °C. The concentration of each of the profilin solution was determined from absorption measurements on a Shimadzu UV-2450 dual beam spectrophotometer using a profilin molar extinction coefficient of $\varepsilon_{280}^{cm-1}=18140$. The OD measurements of the profilin samples containing labeled BODIPY® TMR PPI or BODIPY® FL PI(4,5)P_2 were corrected for the contribution of the labeled PPI at 280 nm.

Anisotropy can be used to determine the dissociation constant of proteins with their ligands [21] Because of the additive property of the anisotropy, the observed anisotropy (r) of a solution containing protein (P) and ligand (L) is given by:

$$r = f_F r_F + f_B r_B \quad (1)$$

where f_F and r_F are the fraction and anisotropy of the ligand free in solution, respectively and f_B and r_B are the fraction and anisotropy of the ligand bound to the protein, respectively. The dissociation constant is given by:

$$K_D = [P]\cdot[L]/[PL] \quad (2)$$

The fraction of the ligand in the bound form can be obtained from:

$$f_B = [PL]/[PL] + [L] = [P]/[P] + K_D \quad (3)$$

Eq. (1) can be rearranged to yield:

$$f_B = r - r_F/r_B - r_F \quad (4)$$

where r_F is obtained by measuring the anisotropy of the ligand in the absence of protein and r_B is measured in presence of a high protein concentration, adequate to bind all ligands. The measured values of r can be used to calculate f_B and f_F and subsequently the dissociation constant for the reaction. One should note that Eq. (4) assumes that there is no change in the quantum yield upon binding which is the case in this study. This is demonstrated by the absence of changes in the lifetime of BODIPY® fluorophores in presence or absence of profilin (Fig. 1).

2.3.3. Förster Resonance Energy Transfer (FRET)

FRET was measured between the BODIPY® FL probes attached to PI(4,5)P_2 excited at 470 nm and the BODIPY® TMR probes attached to PI(4,5)P_2. The FRET efficiency was determined from steady state intensity measurements looking at both the decreased intensity of the donor probe (BODIPY® FL) and the enhancement of the fluorescence intensity of the acceptor probe (BODIPY® TMR). The excitation and emission slits were set at 4 nm. The Förster distance (distance where the efficiency of transfer is 50%) was calculated using:

$$R_0 = 0.2108(n^{-4}Q_d\kappa^2 J)^{1/6} \quad \text{Å} \quad (5)$$

where n is the refractive index of the medium, Q_d is the quantum yield of the donor probe. For BODIPY® FL we used a value of 0.9 [22]. κ^2 is the orientation factor and is assumed to be 2/3 [23]. J is the overlap integral between the fluorescence emission spectrum of the BODIPY® FL PI(4,5)P_2 and the absorption spectrum of BODIPY® TMR PI(4,5)P_2. Using Eq. (5), we calculated an R_0 value for the probe pair of 74 Å.

The efficiency of transfer (E) is related to the distance separating the two probes by:

$$E = R_0^6/R_0^6 + R^6 \quad (6)$$

where R is the distance separating the donor and acceptor probes.

In a solution containing different arrangements of donor acceptor probes, the overall efficiency of transfer is given by:

$$E = \sum \delta_k E_k \quad (7)$$

where δ_k is the probability for the kth arrangement of donor–acceptor probes and E_k the efficiency of transfer for that particular arrangement. The probability δ_k is a function of the acceptor molar fraction (0.5 in this case).

2.3.4. Fluorescence lifetime determinations

The lifetimes of the fluorophores were determined using glycogen scattering as the temporal reference (0 ns). The BODIPY® FL probes were excited at 505 nm while BODIPY® TMR probes were excited at 540 nm. The excitation bandwidth was set to 16 nm. The emission of BODIPY® FL was observed at wavelengths greater than 550 nm through a Melles Griot Schott glass type OG530 cut-off filter and that for BODIPY® TMR was observed at wavelengths greater than 590 nm through a Schott glass type OG570 cut-off filter. The exciting light was polarized vertically (0 °) and the emission polarizer was set to the magic angle (55 °). The phase and modulation data were fit using the Globals software available from the Laboratory for Fluorescence Dynamics at the University of California at Irvine.

2.3.5. Dynamic light scattering

Dynamic light scattering experiments were performed at 25 °C. Detection of the scattered light was performed at 90 ° angle. Prior to dissolving the PI(4,5)P_2, the Milli-Q water was filtered using whatman anatop syringe filters (pores diameter of 0.02 μm). After dilution, the samples were sonicated for 5 min in a Bransonic Ultrasonic cleaner.

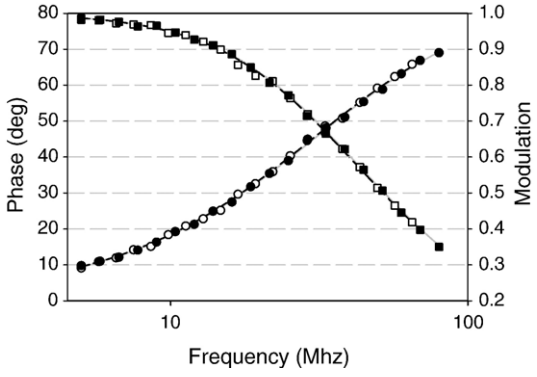

Fig. 1. Multifrequency phase and modulation data obtained for 1 μM BODIPY® TMR PI(4,5)P_2 in presence and absence of profilin. The filled symbols are the phase (●) and modulation (■) data, respectively, measured for BODIPY® TMR PI(4,5)P_2 in absence of profilin. The open symbols represent the phase (○) and modulation (□) data, respectively, determined for BODIPY® TMR PI(4,5)P_2 in presence of 733 μM profilin. The solid lines are the fit of the phase and modulation data.

2.4. Giant unilamellar vesicles (GUVs)

GUV's were prepared using the electroformation method first described by Angelova et al. [24]. The vesicles were formed using POPC and varying amount of PPI lipids (from 0.01% to 10%) on Pt wire electrodes in special chambers described in Fidorra et al. [25]. The lipid mixture was deposited on the Pt wire surface (3 μl of a 0.2 mg/ml lipid stock solution in Cl_3CH/MetOH 2:1 v/v). The sample was then placed under vacuum to remove traces of organic solvent. The vesicles were generated by adding 200 mM sucrose solution and applying a low frequency AC field using a function generator (sine function, 10 Hz, 1.5 V) for 1.5 h at a temperature of 45 °C. The samples were collected and 50 μl of vesicles was added to 250 μl of 200 mM glucose solution in each of the microscopy chambers (Lab-tek Brand Products, Naperville IL). Because of the density differences between the inside and outside of the vesicles, the vesicles sink to the bottom of the chambers few minutes after adding the GUVs into the chamber. Subsequent observation of the GUVs were done in an inverted confocal fluorescence microscope (Zeiss-LSM 510 META NLO, Carl Zeiss, Jena, Germany). The objective used for these experiments was a 40× water immersion with a NA of 1.2. Laser lines at 488 and 543 nm were used for excitation of BODIPY® FL PI(4,5)P_2 and BODIPY® TMR PI(4,5)P_2 respectively. In the FRET experiments excitation was at 488 nm and the observation of the BODIPY-FL fluorescence was through a bandpass BP 510-530IR filter. Time series were obtained for the GUV consisting of 40 images taken with 1.84 s intervals. Two regions of the membrane at the equator of the vesicles were

analyzed together with a region outside the vesicle used for background subtraction. All three regions were of the same size. Changes in the fluorescence intensity with time was recorded for BODIPY® FL PI(4,5)P_2 in presence and absence of BODIPY® TMR PI(4,5)P_2 and profilin.

3. Results

3.1. PI(4,5)P_2 micelles critical concentration

In order to verify that 1 μM of PPI lipids was indeed below the critical micelle concentration, we followed the formation of micelles in solution using light scattering. The concentration of unlabeled PI(4,5)P_2 was varied from 1 μM to 1 mM. While the absorption of the sample varied linearly with the concentration (Fig. 2), the normalized scatter shows no changes in intensity up to 30–40 μM but a sudden decrease in scattering intensity is observed at concentrations above that threshold (Fig. 3A). The 30–40 μM threshold is in very good agreement with the 30 μM critical micelle concentration (CMC) reported for PI(4,5)P_2 lipids by Palmer [26] and is compatible with the CMC estimated by the coomassie blue method of 10 μM by Huang and Huang [27] and the CMC of 12.5 μM obtained using DPH [28] There was no difference in this result using scattering observed at 330 nm or at 350 nm. The decreasing scatter intensity with increasing micelles concentration is attributed to an increased inner filter effect. This inner filter effect is due to the cuvette geometry. Since the light path toward the detector is 2.5 times longer than the light path on the excitation side, the scattered light will have a higher probability of being scattered multiple times after the initial scattering event and therefore would have less chances of reaching the detectors. This would result in a decrease of scattering intensity.

We confirmed these measurements using dynamic light scattering. PI(4,5)P_2 micelles were observed for PI(4,5)P_2 concentrations of 56 μM and 29 μM (Fig. 3B), but the scattering signal was too low to assign any aggregate size for concentration of 21 μM and below. We verified that the absence of assignment was not the result of a lack of sensitivity of the instrument by detecting micelles formed using di-block acrylic acid-8-styrene raft (MW 1648 Da) at a concentration of 6 μM (data not shown).

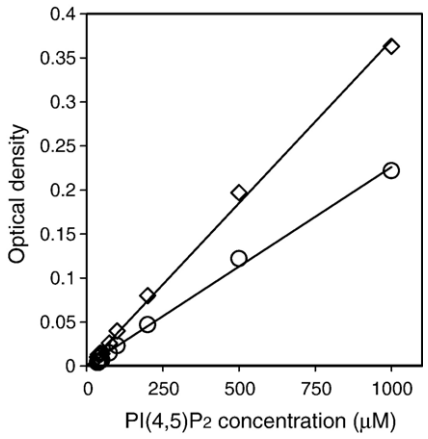

Fig. 2. Changes in optical density of unlabeled PI(4,5)P_2 lipids as a function of concentration. The open diamonds (◊) represent the data obtained at 295 nm. The open circles (○) represent the data obtained at 330 nm. The solid lines are the linear fits of the data.

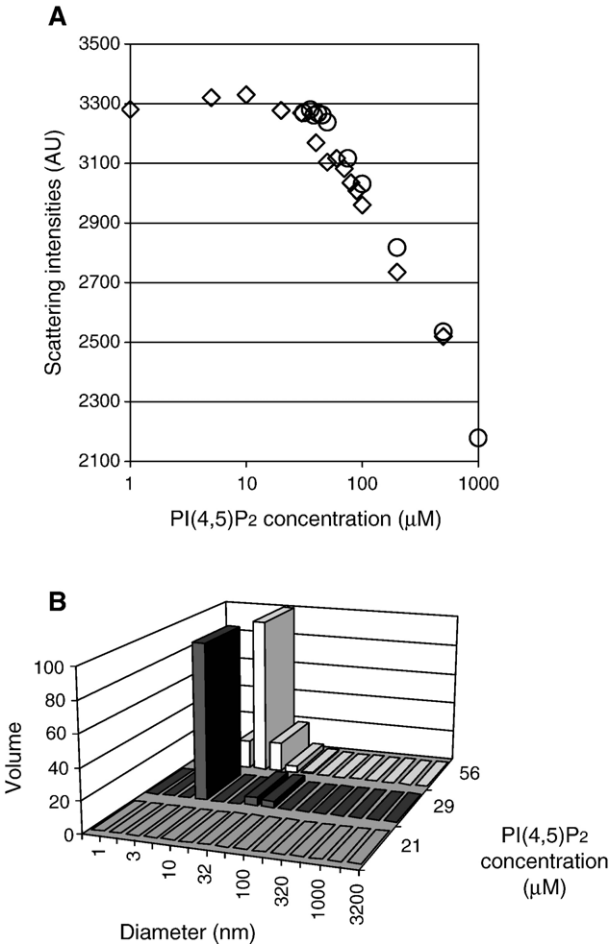

Fig. 3. (A) Effect of PI(4,5)P_2 concentration on the light scattering intensity. The normalized scattering intensities (see Materials and methods) for unlabeled PI(4,5)P_2 were obtained at 330 nm (◊) and 350 nm (○). The breaking point corresponds to concentrations of 30–45 μM. (B) Dynamic light scattering results showing PI(4,5)P_2 aggregate compatible with the size of micelles for 29 μM (black bars) and 56 μM (grey bars) concentrations and no such aggregates at 21 μM (dark grey bars).

We then looked at the anisotropy when the concentration of BODIPY® TMR PI(4,5)P_2 is varied from 500 μM to 1 nM. A very low anisotropy (r) of 0.0245 ± 0.0026 (mean ± stdev) was observed with no concentration dependence (data not shown). Furthermore, the same anisotropy was observed for BODIPY® TMR PI(4,5)P_2:unlabeled PI(4,5)P_2 micelles with molar ratios of 1:100 and 1:1000. This observation suggests that the BODIPY® TMR moiety attached to the sn-1-*O*-acyl chain of the PI(4,5)P_2 molecule interferes with the packing of the lipids in micelles and that the labeled PPI lipids do not incorporate or form micelles at least up to a concentration of 500 μM.

An alternate explanation could be that there is enough disorder in the micelle that the label would freely rotate even when in a micelle. However, this latter explanation is unlikely for the following reasons. For solutions containing a 1:100

molar ratio we will obtain several micelles containing multiple BODIPY® TMR PI(4,5)P_2 molecules. Due to the proximity of the BODIPY® TMR moieties within these micelles and the high R_o value (56.3 Å) for homo-FRET [22], we would expect a high efficiency of homo-FRET to occur. This homo-FRET would result in a decrease in anisotropy [29]. Upon dilution, there would be an increase in anisotropy resulting from a decrease in FRET efficiency. Such increase in anisotropy was not observed.

To further investigate the state of the labeled PI(4,5)P_2 molecules below micellar concentration, we performed hetero-FRET experiments between BODIPY® FL and BODIPY® TMR moieties. We prepared two solutions of 1 μM (1 ml each) of BODIPY® FL PI(4,5)P_2 and BODIPY® TMR PI(4,5)P_2, respectively. The emission spectrum of these two solutions were recorded and these two spectra (without FRET) were added (Fig. 4A). This was followed by the addition of 1 μL of a 1 mM solution of the BODIPY® TMR PI(4,5)P_2 or the BODIPY® FL PI(4,5)P_2 in the BODIPY® FL PI(4,5)P_2 and BODIPY® TMR PI(4,5)P_2 solutions, respectively. The emission spectrum of BODIPY® TMR PI(4,5)P_2-BODIPY® FL PI(4,5)P_2 and BODIPY® FL PI(4,5)P_2- BODIPY® TMR PI(4,5)P_2 solutions were then recorded. No significant changes in intensities of the donor could be detected (Fig. 4B) in either solutions. A small increase of the emission of the BODIPY® FL PI(4,5)P_2-BODIPY® TMR PI(4,5)P_2 sample was observed (4%). However, since this is not correlated with a decrease in the donor emission, it probably results from the addition of concentrated BODIPY-TMR PI(4,5)P_2 to the BODIPY® FL PI(4,5)P_2 solution. The absence of FRET demonstrate that for concentrations of 2 μM labeled PI(4,5)P_2, the molecules do not form aggregates and are mostly mono-dispersed. Indeed, in the case of a dimer, assuming a random association of the BODIPY® FL PI(4,5)P_2 and BODIPY® TMR PI(4,5)P_2 molecules, we will have three population of dimers, one with donor probes only, one with acceptor probes only and the third one with donor–acceptor probes. Only the donor–acceptor solutions will results in FRET efficiency. Assuming a molecule length of ~40 Å, and using Eq. (6), we can calculate the expected efficiency of transfer for these dimers. If the monomers in the dimer are parallel, the efficiency of transfer would be >99% while if the monomers are anti-parallel, the efficiency of transfer would be >97%. The probability of the mixed donor–acceptor probe dimers is 50% when the same concentration of acceptor and donor labeled lipids are mixed in equal amount. Using Eq. (7), the expected efficiency of energy transfer for the solution would be ~50% if the monomers in the dimers are parallel and ~48% if the monomers in the dimers are anti-parallel, i.e. with the probes on opposite side of the dimers. Higher aggregates for instance tetramers would result in even more FRET [30]. Since we could not detect FRET, we can conclude that most if not all of the labeled PI(4,5)P_2 lipids are mono-dispersed and do not form aggregates at concentrations below 2 μM. However, this finding may not be true for the unlabeled PI(4,5)P_2 which might form aggregates at these concentrations since they have longer fatty acid chains and are less water soluble than the BODIPY labeled PPI.

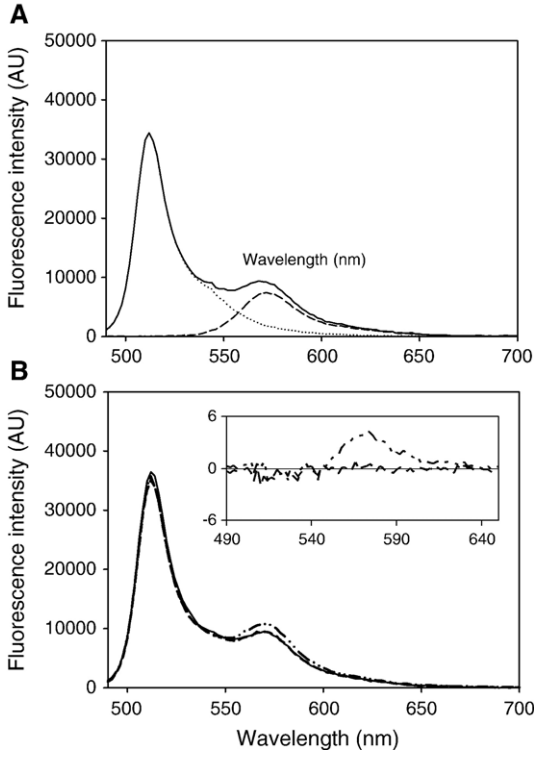

Fig. 4. Steady state fluorescence intensity of BODIPY® FL PI(4,5)P_2 and BODIPY® TMR PI(4,5)P_2. (A) Dotted line (···): Fluorescence emission spectrum of 1 μM BODIPY® FL PI(4,5)P_2. The fluorescence emission spectrum of 1 μM BODIPY® TMR PI(4,5)P_2 is represented by the dashed line (– – –). The solid line is the sum of the two spectra. (B) FRET efficiency between the acceptor and donor labeled PIP(4,5)P_2. The dashed line (– – –) represents the spectrum obtained for BODIPY® TMR PI(4,5)P_2-BODIPY® FL PI(4,5)P_2. The dot-dot-dashed line (· · –) represents the spectrum obtained for BODIPY® FL PI(4,5)P_2-BODIPY® TMR PI(4,5)P_2. The solid line is the sum of the two spectra without FRET from **A.** above. The insert is the differential in % between the sum of the two spectra without FRET and BODIPY® TMR PI(4,5)P_2-BODIPY® FL PI(4,5)P_2, dashed line (– – –) and BODIPY® FL PI(4,5)P_2-BODIPY® TMR PI(4,5)P_2, dot-dot-dashed line (· · –).

3.2. Anisotropy of PPI:profilin complex

The anisotropy data for BODIPY® TMR PI(4,5)P_2 and BODIPY® TMR PI(3,4,5)P_3 in the presence of profilin at concentrations ranging from 6 μM to 950 μM are presented in Fig. 5. The data obtained with profilin from outdated platelets or from the expression of Human profilin in bacteria were similar and therefore were considered together. The anisotropy of the PPI:profilin complexes decreased with decreasing profilin concentration and reached values similar to the anisotropy of the free BODIPY® TMR PI(4,5)P_2. We also note that the anisotropy values for the BODIPY® TMR PI(3,4,5)P_3:profilin complexes are higher than those obtained for BODIPY® TMR PI(4,5)P_2 suggesting a lower dissociation constant for PI(3,4,5)P_3.

To ascertain that the binding is not due to the BODIPY® TMR probe interacting directly with profilin, the anisotropy of another labeled phosphoinositide was measured complexed with profilin: BODIPY® FL PI(4,5)P_2. Having very different chemistry, it is unlikely that the fluorescent labels i.e. BODIPY®

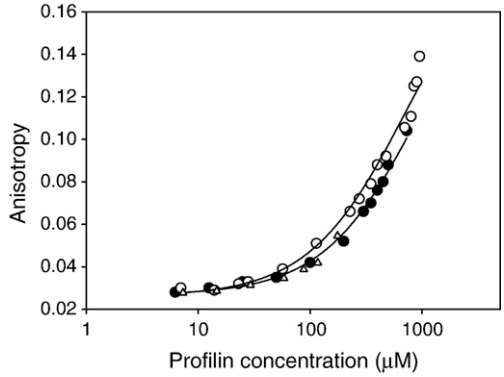

Fig. 5. Anisotropy data for the binding of BODIPY® TMR labeled PPI lipids with profilin. The labeled PPI concentration was kept constant at 1 μM. The filled circles (●) are the data obtained for BODIPY® TMR PI(4,5)P_2. The open triangles (△) are the data obtained for BODIPY® TMR PI(4,5)P_2 using profilin purified from Human platelets. The open circles (○) represent the data obtained with BODIPY® TMR PI(3,4,5)P_3. The solid lines are the fit of the data using an estimated anisotropy value for the lipid bound to profilin of 0.20. The calculated K_Ds are 985 μM (r^2=0.993) and 720 μM (r^2=0.983) for BODIPY® TMR PI(4,5)P_2 and BODIPY® TMR PI(3,4,5)P_3, respectively.

TMR and BODIPY® FL, would bind profilin with the same affinity. These results are presented in Fig. 6. It is clear that the concentration range at which profilin binds to the PPI lipids is the same independent of the fluorophores.

We also verified that profilin does not form aggregates at high concentration which would result in an overestimation of the anisotropy of the PPI/profilin complex. We determined the anisotropy of profilin alone using the fluorescence of the intrinsic tryptophan and could not detect any increase of the anisotropy (mean±SEM; 0.0667±0.0012) up to 840 μM. A slight increase in anisotropy is detected for higher concentration (r=0.0772 for 1650 μM profilin) which indicate that profilin starts to form aggregates at concentrations higher than 840 μM. This formation of aggregates could modify the observed anisotropy in two ways. If the aggregation does not prevent the binding of mono-dispersed PPI to profilin, the anisotropy would be overestimated. This could explain the slight deviation of the anisotropy from the fitted curve for the binding of mono-dispersed PI(3,4,5)P_3 with high concentration of profilin (Fig. 5, open circle last point). If on the other hand the aggregation of profilin prevents the binding of mono-dispersed PPI, then the observed anisotropy should decrease to a plateau. Such a decrease was not observed.

In order to determine the dissociation constant (K_D) of the PPI/profilin complex, the anisotropy of BODIPY® TMR bound to PPI must be determined. However, to achieve nearly complete binding, profilin concentrations would have to be at least a factor of 10 higher than that available here. This value was thus estimated as described below. The correct quantitative relation between the polarization, the excited state lifetime, the size of the fluorophore and the viscosity of the medium was described by F. Perrin in 1926 [31] [for a recent review see Jameson et al. [29]].

The Perrin equation in terms of anisotropy is:

$$r_0/r = (1 + \tau/\tau_c) \quad (8)$$

Where r is the anisotropy, r_0 is the limiting anisotropy (in absence of rotation), τ is the excited state lifetime of the fluorophore and τ_c the rotational correlation time.

Assuming that the molecule is spherical, τ_c is equal to:

$$\tau_c = \eta M(\upsilon + h)/RT \quad (9)$$

where η is the viscosity of the medium, M is the molecular weight, υ is the partial specific volume, h the degree of hydration, R is the universal gas constant and T the absolute temperature. Using the molecular weight of the profilin PPI lipid complex, the rotational correlation time can be estimated to be ~7 ns for BODIPY® TMR PI(4,5)P_2 and BODIPY® TMR PI(3,4,5)P_3 and ~6.6 ns for BODIPY® FL PI(4,5)P_2. The limiting anisotropies of the probes were determined using 1 μM of labeled PPI lipids in anhydrous glycerol at 0 °C. Values of 0.365±0.001 and 0.353±0.002 were obtained for BODIPY® TMR PI(4,5)P_2 and BODIPY® FL PI(4,5)P_2, respectively.

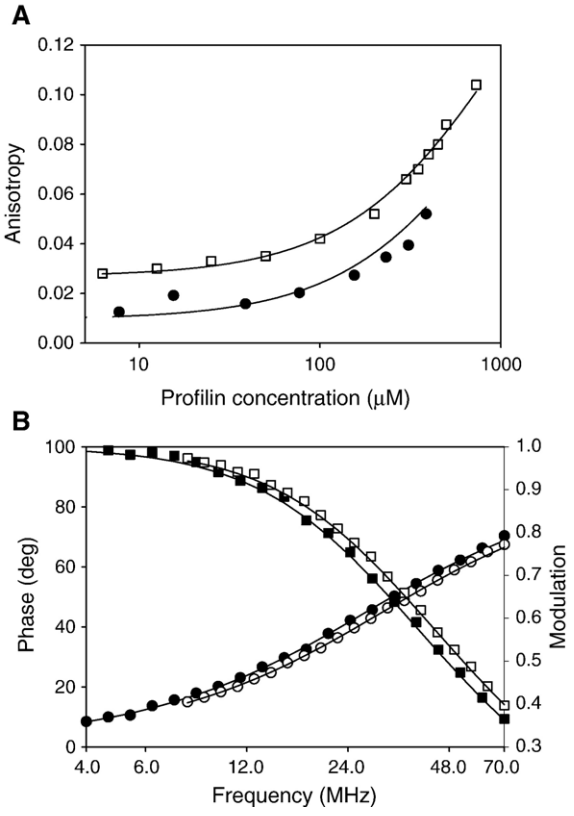

Fig. 6. (A) Anisotropy data for the binding of BODIPY® TMR PI(4,5)P_2 and BODIPY® FL PI(4,5)P_2 with profilin. The labeled PPI concentration was kept constant at 1μM. The open squares (□) represent the data obtained for BODIPY® TMR PI(4,5)P_2 while the filled circles (●) are the data obtained for BODIPY® FL PI(4,5)P_2. Lower anisotropy values are the results of a combination of lower molecular size and longer lifetime. The solid lines are the fit of the data using a K_D value of 985 μM. (B) Multifrequency phase and modulation data obtained for BODIPY® TMR PI(4,5)P_2 and BODIPY® FL PI (4,5)P_2. The filled symbols are the phase (●) and modulation (■) data, respectively, measured for BODIPY® TMR PI(4,5)P_2. The open symbols represent the phase (○) and modulation (□) data, respectively, determined for BODIPY® FL PI(4,5)P_2. The solid lines are the fit of the phase and modulation data.

These values are in very good agreement with the limiting anisotropy value of 0.37 reported by Karolin et al. [32]. One more parameter needs to be measure in order to estimate the anisotropy value of the bound labeled PPI, namely the lifetimes of the BODIPY® TMR and BODIPY® FL labeled phospholipids.

3.3. Lifetimes of BODIPY® TMR PI(4,5)P_2 and BODIPY® FL PI(4,5)P_2

The lifetimes of the two fluorophores were measured both with the PPI free in solution and bound with 387 μM of profilin for BODIPY® FL PI(4,5)P_2 and 733 μM of profilin for BODIPY® TMR PI(4,5)P_2. In each case, the best fit was always obtained for a single discrete exponential decay. Furthermore, there are no differences in lifetimes between the labeled phospholipids free in solution or bound to profilin (Fig. 1). The data for the lifetimes of BODIPY® TMR PI(4,5)P_2 and BODIPY® FL PI(4,5)P_2 are shown in Fig. 6B. A lifetime value of 5.1 ns (χ^2=3.5) was obtained for BODIPY® TMR and a slightly longer lifetime of 5.9 ns (χ^2=6.4) was obtained for BODIPY® FL. Reduced χ^2 values were calculated using nonlinear least-squares analysis assuming standard phase and modulation errors of 0.2° and 0.004, respectively, as described in Jameson et al. [33] These lifetimes are in good agreement with those reported by Karolin et al. [32].

3.4. Dissociation constant of the labeled PPI

Using the Perrin equation, a value of 0.20±0.05 was then estimated for the anisotropy of the BODIPY® TMR PPI bound to profilin and a value of 0.18±0.05 for the anisotropy of the BODIPY® FL PPI bound to profilin.

The data from Figs. 5 and 6A were fit using nonlinear curve fitting (SigmaPlot) and dissociation constants of labeled PPI with profilin were obtained. The solid lines in Fig. 5 represent the fit for K_D values of 720±40 μM and 985±40 μM for submicellar concentration of PI(3,4,5)P_3 and PI(4,5)P_2, respectively. The curve fitting on Fig. 6A was obtained with the PI(4,5)P_2 K_D value of 985 μM.

3.5. Binding of profilin to BODIPY® TMR PI(4,5)P_2 and BODIPY® FL PI(4,5)P_2 in a membrane model system: the GUV

In order to test that despite the low binding affinity of profilin for submicellar concentration of PPI, profilin bind to the BODIPY® labeled lipids incorporated in a membrane, we investigated the changes in FRET between BODIPY® FL PI(4,5)P_2 and BODIPY® TMR PI(4,5)P_2 in GUVs composed of POPC. GUV's have at least two advantages over micelles, small unilamellar vesicles and large unilamellar vesicles. They have a membrane curvature similar to cells and they are visible in the microscope.

Both BODIPY® FL PI(4,5)P_2 and BODIPY® TMR PI(4,5)P_2 do not partition easily into the POPC membrane. Partitioning was only obtained for 1% BODIPY® FL PI(4,5)P_2 and 0.1% BODIPY® TMR PI(4,5)P_2 (Fig. 7A, B). When BODIPY® FL PI(4,5)P_2 and BODIPY® TMR PI(4,5)P_2 were both present in the membrane, partitioning was obtained for 0.25% of each of the labeled lipid. Also, when GUV's were formed of POPC/unlabeled PI(4,5)P_2 10:1 mol, the labeled PI(4,5)P_2 did not partitioned to the membrane (Fig. 7C). Lack of partitioning of these short (C6) BODIPY® labeled PPI to the membrane has been previously reported by Cho et al. who noticed that these lipids were not well localized to the surface membrane and were equally found in the cytoplasm [34].

Donor photobleaching [35] was used to investigate the FRET between the BODIPY® labeled lipids in the GUV. Due to the large R_0 values for either homo-FRET or hetero-FRET (>50 Å) and at the lipids concentration used, FRET and hence resistance of the BODIPY® FL PI(4,5)P_2 to photobleaching is present even in absence of profilin. Quantification of the FRET efficiency was however not possible. Indeed, in order to quantify the FRET efficiency, one needs to obtain on the same vesicle the bleaching rate of the donor labeled lipid only. It is possible to achieve this by photobleaching the acceptor probe and then looking at the rate of photobleaching of the donor in two areas of the membrane; one where the acceptor is present and one where the acceptor has been photobleached. The latter gives the rate of photobleaching for the donor labeled lipid only. However, due to the high diffusion rates of the BODIPY®

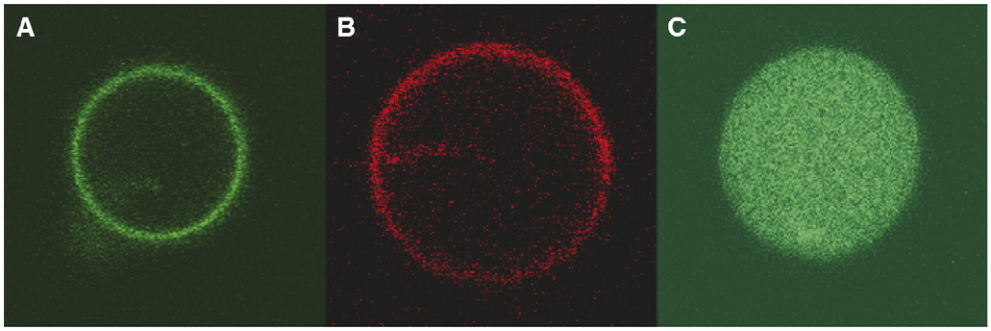

Fig. 7. Partitioning of the BODIPY® FL PI(4,5)P_2 and BODIPY® TMR PI(4,5)P_2 in the POPC GUVs. (A) POPC GUV containing 1 mol% BODIPY® FL PI(4,5)P_2. (B) POPC GUV containing 0.1 mol% BODIPY® TMR PI(4,5)P_2. (C) GUV formed of POPC/unlabeled PI(4,5)P2 10:1 mol with 1 mol% BODIPY® FL PI(4,5)P_2. The three pictures are taken at the equatorial plane of the vesicles.

labeled lipids and the lack of compartmentalization of the GUV, the bleaching of the acceptor labeled lipid was not possible. Also, because of the different donor labeled $PI(4,5)P_2$ concentration between the GUV's containing donor only (1%) and donor in presence of acceptor (0.25%), it was not possible to obtain the rate of photobleaching of the donor only at 0.25%

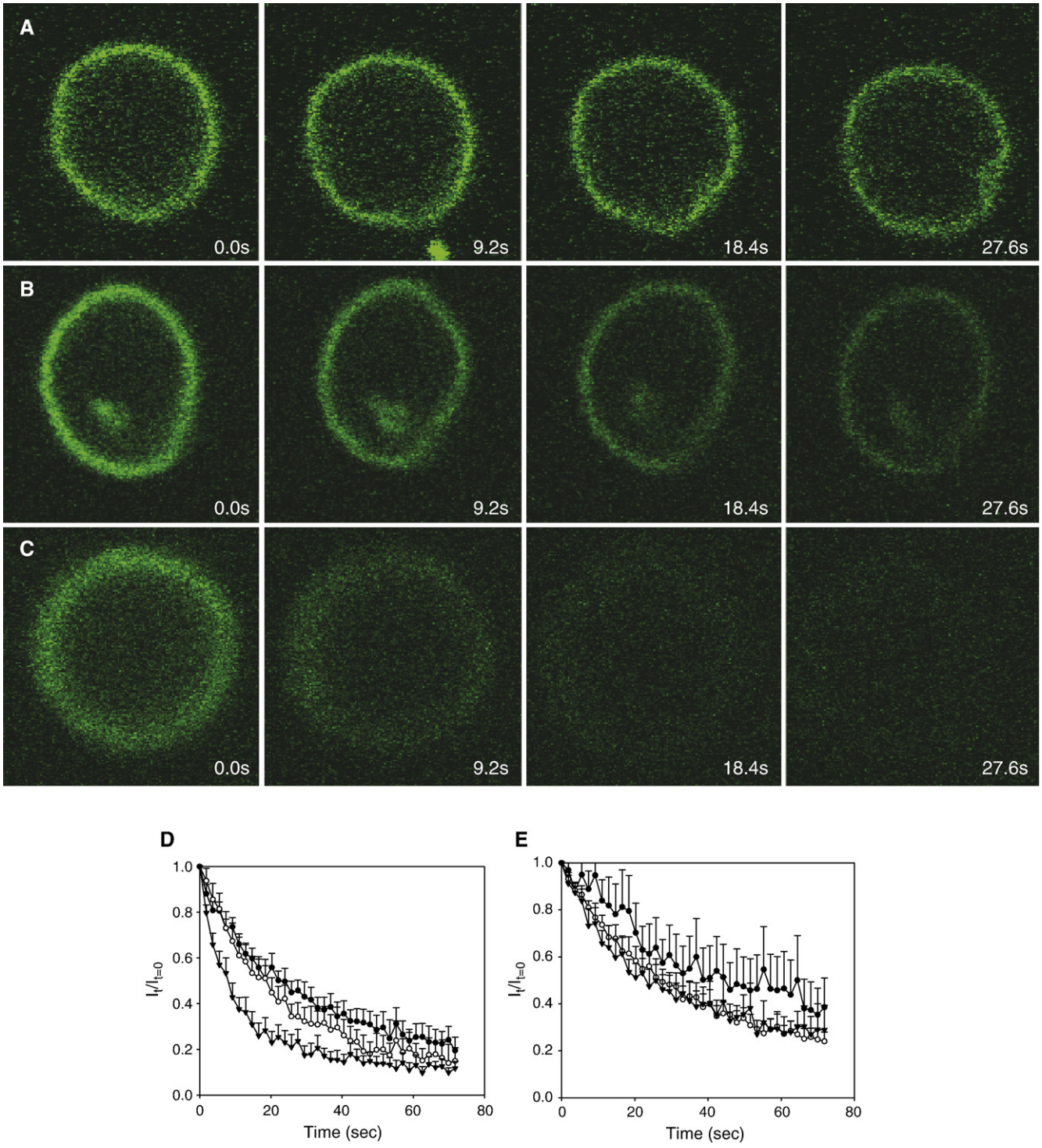

Fig. 8. Effect of profilin binding to the photobleaching rate of BODIPY® FL $PI(4,5)P_2$. (A) Photobleaching of the POPC GUV containing 0.25% BODIPY® FL $PI(4,5)P_2$ and 0.25% BODIPY® TMR $PI(4,5)P_2$ in absence of profilin. (B) Photobleaching of the GUV showed in panel A in presence of 20 μM profilin. (C) Photobleaching of the GUV showed in panel A in presence of 90 μM profilin. (D) Decrease in fluorescence intensity of the BODIPY® FL $PI(4,5)P_2$ as a function of time for a POPC GUV containing 0.25% BODIPY® FL $PI(4,5)P_2$ and 0.25% BODIPY® TMR $PI(4,5)P_2$. (E) Decrease in fluorescence intensity of the BODIPY® FL $PI(4,5)P_2$ as a function of time for a POPC GUV containing 1% BODIPY® FL $PI(4,5)P_2$. The filled circles (●) are the data obtained in absence of profilin. The open circles (○) are the data obtained for the GUVs in presence of 20 μM profilin and the filled triangles (▼) are the data obtained for the GUVs in presence of 90 μM profilin. The error bars are the SEM.

as the efficiency of homo-FRET is different in both cases. Therefore, the data were only analyzed qualitatively. Fig. 8 shows the rate of the donor labeled PI(4,5)P_2 photobleaching in absence and presence of profilin for donor only and donor with acceptor labeled PI(4,5)P_2. There is a clear increase in the BODIPY® FL PI(4,5)P_2 rate of photobleaching in presence of profilin and this change is larger at higher profilin concentration (90 μM) showing that profilin interact with the labeled PI(4,5)P_2 in the GUV lipid bilayer.

4. Discussion

In the last 15 years, several authors studied the binding of profilin to PI(4,5)P_2 and/or PI(3,4,5)P_3 micelles using the changes in fluorescence intensity of profilin's tryptophan upon PPI binding [15,18,36]. Our scattering data were obtained at the wavelength corresponding to the emission wavelength of tryptophan residues used in these previous studies. We showed in this paper that above the critical micelle concentration of around 30 μM, there is an increased inner filter effect with the increase in PI(4,5)P_2 concentration. Therefore, we can expect that at least part of the decrease of the tryptophan fluorescence observed upon increased concentration of PPI micelles will be due to this inner filter effect. In the present study, we used cuvettes with a shorter path length than the conventional 10×10 mm cuvette. The sizes of the cuvettes used in the previous studies are unfortunately not reported. However, if these fluorescence intensity experiments were done in 10×10 mm cuvettes, then the inner filter effect reported here would be even larger.

Some of the previous binding experiments between profilin and PPI micelles, were obtained using a range of PPI concentrations that overlapped the transition between sub-micellar and micellar lipids [15,36] i.e. ranging from 0.5 to 95 μM [15] and from 9 to 45 μM PI(4,5)P_2 [36]. The overlap with the micellar transition would probably not be an issue if the dissociation constant between sub-micellar concentration of PPI lipids and profilin was the same as the dissociation constant obtained with micellar PPI lipids. Since there is at least a 30 fold difference in the dissociation constant between profilin and micellar or sub-micellar concentration of PPI lipids, these published data cannot be used to determine the dissociation constant between profilin and PI(4,5)P_2 or PI(3,4,5)P_3 micelles. Indeed, the data will be contaminated with the low binding affinity for sub-micellar lipids as well as with the transition phase into micelles.

From our experiments, it is difficult to determine whether the interaction between profilin and the PPI lipids occur through the hydrophobic tail or the negatively charged head of the phospholipids. However, we can probably exclude the interaction of profilin with the fluorophore moiety. Indeed, we do not detect any changes in the fluorescence lifetimes and therefore quantum yields of the two fluorophores used when profilin binds to the PPI. Also, in the case of binding to the fluorophore, we would expect to obtain a different dissociation constant between the BODIPY® TMR PI(4,5)P_2 and BODIPY® FL PI(4,5)P_2 due to the different chemistry of the fluorophores. Such a difference was not observed. The difference in anisotropy for the BODIPY® FL PI(4,5)P_2 compared to BODIPY® TMR PI(4,5)P_2 is due to a smaller size of the molecule together with the longer lifetime of the fluorophore.

In addition, our data demonstrate a lower dissociation constant for BODIPY® TMR PI(3,4,5)P_3 compared to BODIPY® TMR PI(4,5)P_2, which strongly suggests that profilin is indeed interacting with the negatively charged phosphates of the phospholipids heads and not with the hydrophobic tail or the fluorophore.

In our estimation of the anisotropy of lipids bound to profilin (r_B), we assumed a spherical protein lipid complex. Jameson and Seifried [37], discussed the effect on the polarization/anisotropy when the shape of the molecule deviates from the spherical model. Such deviation would result in an increased value of the polarization/anisotropy of the complex and therefore an increased value of the dissociation constant.

Lassing and Lindberg initially showed that the packing of the lipid can determine the efficiency of the dissociation of the profilin:actin complex by PI(4,5)P_2 [38]. Also, these authors, in one of their early works on the interaction between profilin:actin and PI(4,5)P_2 [16], showed that in their experimental conditions soluble inositol (1,4,5) trisphosphate did not dissociate the profilin:actin complex and did not prevent the dissociation of the profilin:actin complex by PI(4,5)P_2. Lassing and Lindberg suggested that in order to form a stable complex, profilin has to interact with the phosphorylated inositols of at least two adjacent PPI molecules. Later, Goldschmidt-Clermont et al. [17] demonstrated using large unilamellar vesicles (LUVET), that each profilin molecules protected approximately 5 PI(4,5)P_2 molecules from hydrolysis by phospholipase C. These authors proposed that profilin could aggregate PI(4,5)P_2 into small patches. Our data support the hypothesis that the initial interaction of profilin with the PPI lipids could require more that one PPI and/or that the membrane is an essential component of the profilin interaction with PPI. Our GUV data also suggest that profilin is able to recruit adjacent PPI lipids. Indeed, as illustrated by the schematic drawing in Fig. 9, in absence of profilin, the donor and acceptor labeled PPI could be distributed across the membrane (Fig. 9A). As the R_0 value for the probe pair is around 74 Å, this would result in a significant level of FRET thus partially protecting the donor from photobleaching. When profilin is added, recruitment of PPI by profilin will have two effects (Fig. 9B). Firstly, the efficiency of transfer between the labeled PPI clustered around profilin would dramatically increase to >90%, thus protecting the donor from photobleaching but also reducing the donor fluorescence intensity dramatically. Secondly, the donor labeled PPI that are not recruited by profilin will have a reduction in FRET efficiency, resulting in higher initial fluorescence intensity but also a much higher susceptibility to photobleaching. This model could explain the biphasic shape of the donor photobleaching curve observe in presence of profilin in Fig. 8. Also, in the case of the donor only control there is initially more BODIPY® FL labeled PI(4,5)P_2 in the membrane; 1% compared to 0.25%, which would result in homo-FRET, thus protecting the BODIPY® FL labeled PI(4,5)P_2 from photobleaching. In presence of profilin,

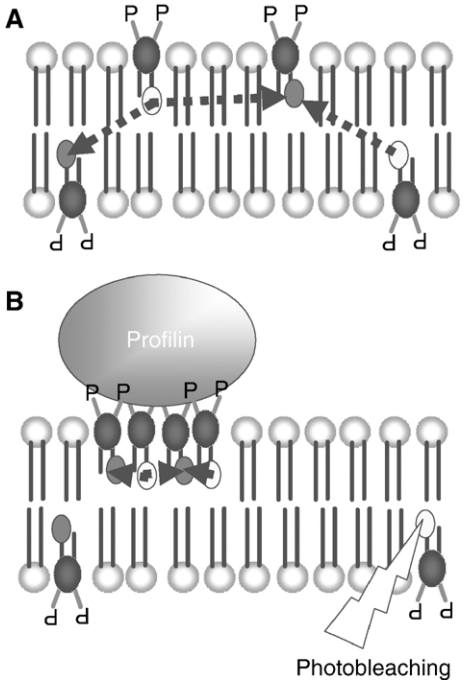

Fig. 9. Model of profilin interaction with the BODIPY® labeled PI(4,5)P_2. (A) In absence of profilin, the BODIPY® labeled PI(4,5)P_2 are distributed randomly in the leaflets of the lipid bilayer. Due to the large R_0 values for the probe pairs, FRET (represented by the dotted arrows) occurs between the donor and acceptor probes, protecting the donor from photobleaching. (B) In presence of profilin, the BODIPY® labeled PI(4,5)P_2 are clustered by profilin increasing the FRET efficiency between the donor and acceptor in the cluster to >90% resulting in a large decrease in donor intensity. The clustering isolates some of the donor labeled PI(4,5)P_2 which do not participate in FRET anymore, the initial intensity of these donor probes is higher but they are now much more susceptible to photobleaching.

the fluorescence intensity of the donor only GUV do not decrease as dramatically as observed for the GUV containing both BODIPY® FL PI(4,5)P_2 and BODIPY® TMR PI(4,5)P_2 because of the significant homo-FRET in the cluster.

Studies on Gelsolin, another PI(4,5)P_2 binding protein has been shown to depend on the mole fraction of PI(4,5)P_2 in phosphatidylcholine vesicles [39,40].When the mole fraction of PI(4,5)P_2 fall below 5 to 10% of the membrane lipids composition, Gelsolin becomes insensitive to PI(4,5)P_2. This is in contrast with the results obtained with GUV and profilin. Indeed, binding of profilin to the PI(4,5)P_2 in the GUV membrane was observe for a molar fraction of PI(4,5)P_2 of only 0.5% of the lipids in the GUVs. This could reflect a difference in the mechanism of interaction between the PPI and the two proteins, profilin and gelsolin or a difference inherent of the model system used, GUV compared to liposomes.

Ostrander et al. [12] reported that, in yeast, profilin binding to PI(4,5)P_2 lipids followed surface dilution kinetics. These authors examined the dependence of the surface concentration of PI(4,5)P_2 and found that the binding of profilin was indeed dependent on the surface concentration and that this binding appeared cooperative with a Hill coefficient of 2.

Since in human erythrocytes, the PI(4,5)P_2 lipids is thought to represent only 1% of the total lipids of the membrane [41], the difference in binding between profilin and gelsolin may have physiological significance. Indeed, PI(4,5)P_2 clusters could be essential to allow interactions with proteins such as gelsolin but might not be so crucial for profilin. In *Acanthamoeba castellanii*, immunofluorescence experiments localized PI(4,5)P_2 associated with the plasma membrane and particularly at the leading edge of migrating cells [42]. Such localization to specific regions of the cells, would result in a local increase in PI(4,5)P_2 concentration which might be sufficient to induce the initial association of profilin to PPI lipids. High local concentrations of PI(4,5)P_2 could also arise from the localized production of PI(4,5)P_2 by the type I PIP kinases [43,44]. Using pleckstrin-homology (PH) domain fused to green fluorescent protein (GFP) as a probe for PI(4,5)P_2 in NIH-3T3 fibroblasts Tall et al. [45] revealed intense, non-uniform fluorescence in distinct structures at the cell periphery. These authors identified these structures as ruffles and microvillus-like protrusions. Doughman et al. suggested that these local increase in PI(4,5)P_2 levels induces actin remodeling [44]. These local enrichments of PI(4,5)P_2 might be sufficient to allow for the binding of profilin to the membrane and the sequestration of PI(4,5)P_2 by profilin or *vice versa*. Profilin:actin after catalyzing the exchange of ADP for ATP in the actin cleft, could bind to PI(4,5)P_2. The recruitment of additional PI(4,5)P_2 by profilin would release actin from profilin which can then be incorporated into growing actin filaments. Profilin remaining bond to the PI(4,5)P_2 lipids, would then protect PI(4,5)P_2 from hydrolysis by phospholipase C-γ1 [17].

The data presented here, clearly demonstrate the need for a better understanding of the processes driving the binding of profilin to the membrane and the factors that could affect this association. Experiments are underway to address these questions.

Acknowledgements

The authors thank Prof. David M. Jameson and Prof. William H. Sawyer for their helpful comments and discussions. We also thank Dr. Hank De Bruyn, Dr. Desislava Ganeva and the staff of the Key Centre for Polymer Colloids at the University of Sydney (Australia) for their help with the dynamic light scattering experiments. This work was supported by a University Research Grant (RE211241) from the University of New England (Australia), a Linkage Infrastructure Equipment and Facilities Grant (LE0561041) from the Australian Research Council (ARC) and a grant from the ARC/NHMRC Fluorescence Application in Biotechnology and Life Sciences network (RN0460002). Research in the laboratory of L. A. B. is funded by a grant from SNF, Denmark (21-03-0569) and the Danish National Research Foundation (which supports MEMPHYS-Center for Biomembrane Physics).

References

[1] L. Carlsson, L.E. Nystrom, I. Sundkvist, F. Markey, U. Lindberg, Actin polymerizability is influenced by profilin, a low molecular weight protein in non-muscle cells, J. Mol. Biol. 115 (1977) 465–483.
[2] E. Reichstein, E.D. Korn, *Acanthamoeba profilin*. A protein of low

molecular weight from *Acanpthamoeba castellanii* that inhibits actin nucleation, J. Biol. Chem. 254 (1979) 6174–6179.
[3] R. Valenta, M. Duchene, C. Ebner, P. Valent, C. Sillaber, P. Deviller, F. Ferreira, M. Tejkl, H. Edelmann, D. Kraft, O. Scheiner, Profilins constitute a novel family of functional plant pan-allergens, J. Exp. Med. 175 (1992) 377–385.
[4] L.M. Machesky, N.B. Cole, B. Moss, T.D. Pollard, Vaccinia virus expresses a novel profilin with a higher affinity for polyphosphoinositides than actin, Biochemistry 33 (1994) 10815–10824.
[5] M. Haugwitz, A.A. Noegel, J. Karakesisoglou, M. Schleicher, Dictyostelium amoebae that lack G-actin-sequestering profilins show defects in F-actin content, cytokinesis, and development, Cell 79 (1994) 303–314.
[6] W. Witke, J.D. Sutherland, A. Sharpe, M. Arai, D.J. Kwiatkowski, Profilin I is essential for cell survival and cell division in early mouse development, Proc. Natl. Acad. Sci. U. S. A. 98 (2001) 3832–3836.
[7] A. Lambrechts, V. Jonckheere, D. Dewitte, J. Vandekerckhove, C. Ampe, Mutational analysis of human profilin I reveals a second PI(4,5)-P2 binding site neighbouring the poly(L-proline) binding site, BMC Biochem. 3 (2002) 1–12.
[8] P.J. Goldschmidt-Clermont, L.M. Machesky, S.K. Doberstein, T.D. Pollard, Mechanism of the interaction of human platelet profilin with actin, J. Cell Biol. 113 (1991) 1081–1089.
[9] L.S. Tobacman, E.D. Korn, The regulation of actin polymerization and the inhibition of monomeric actin ATPase activity by *Acanthamoeba profilin*, J. Biol. Chem. 257 (1982) 4166–4170.
[10] E. Korenbaum, P. Nordberg, C. Bjorkegren-Sjogren, C.E. Schutt, U. Lindberg, R. Karlsson, The role of profilin in actin polymerization and nucleotide exchange, Biochemistry 37 (1998) 9274–9283.
[11] C.G. dos Remedios, D. Chhabra, M. Kekic, I.V. Dedova, M. Tsubakihara, D.A. Berry, N.J. Nosworthy, Actin binding proteins: regulation of cytoskeletal microfilaments, Physiol. Rev. 83 (2003) 433–473.
[12] D.B. Ostrander, J.A. Gorman, G.M. Carman, Regulation of profilin localization in *Saccharomyces cerevisiae* by phosphoinositide metabolism, J. Biol. Chem. 270 (1995) 27045–27050.
[13] J.H. Hartwig, K.A. Chambers, K.L. Hopcia, D.J. Kwiatkowski, Association of profilin with filament-free regions of human leukocyte and platelet membranes and reversible membrane binding during platelet activation, J. Cell Biol. 109 (1989) 1571–1579.
[14] P.J. Goldschmidt-Clermont, J.W. Kim, L.M. Machesky, S.G. Rhee, T.D. Pollard, Regulation of phospholipase C-gamma 1 by profilin and tyrosine phosphorylation, Science 251 (1991) 1231–1233.
[15] P.J. Lu, W.R. Shieh, S.G. Rhee, H.L. Yin, C.S. Chen, Lipid products of phosphoinositide 3-kinase bind human profilin with high affinity, Biochemistry 35 (1996) 14027–14034.
[16] I. Lassing, U. Lindberg, Specificity of the interaction between phosphatidylinositol 4,5-bisphosphate and the profilin:actin complex, J. Cell. Biochem. 37 (1988) 255–267.
[17] P.J. Goldschmidt-Clermont, L.M. Machesky, J.J. Baldassare, T.D. Pollard, The actin-binding protein profilin binds to PIP2 and inhibits its hydrolysis by phospholipase C, Science 247 (1990) 1575–1578.
[18] V. Raghunathan, P. Mowery, M. Rozycki, U. Lindberg, C. Schutt, Structural changes in profilin accompany its binding to phosphatidylinositol, 4,5-bisphosphate, FEBS Lett. 297 (1992) 46–50.
[19] P. Skare, R. Karlsson, Evidence for two interaction regions for phosphatidylinositol(4,5)- bisphosphate on mammalian profilin I, FEBS Lett. 522 (2002) 119–124.
[20] P.A. Janmey, Polyproline affinity method for purification of platelet profilin and modification with pyrene-maleimide, Methods Enzymol. 196 (1991) 92–99.
[21] S.Y. Tetin, T.L. Hazlett, Optical spectroscopy in studies of antibody-hapten interactions, Methods 20 (2000) 341–361.
[22] I.D. Johnson, H.C. Kang, R.P. Haugland, Fluorescent membrane probes incorporating dipyrromethene boron difluoride fluorophores, Anal. Biochem. 198 (1991) 228–237.
[23] C.G. dos Remedios, P.D. Moens, Fluorescence resonance energy transfer spectroscopy is a reliable "ruler" for measuring structural changes in proteins. Dispelling the problem of the unknown orientation factor, J. Struct. Biol. 115 (1995) 175–185.
[24] M.I. Angelova, S. Soleau, P. Meleard, J.F. Faucon, P. Bothorel, Preparation of giant vesicles by external AC fields. Kinetics and application, Prog. Colloid Polym. Sci. 89 (1992) 127–131.
[25] M. Fidorra, L. Duelund, C. Leidy, A. Simonsen, L.A. Bagatolli, Absence of fluid-ordered/fluid-disordered phase coexistence in ceramide/POPC mixtures containing cholesterol, Biophys. J. 90 (2006) 4437–4451.
[26] F.B. Palmer, The phosphatidyl-myo-inositol-4,5-biphosphate phosphatase from *Crithidia fasciculata*, Can. J. Biochem. 59 (1981) 469–476.
[27] F.L. Huang, K.P. Huang, Interaction of protein kinase C isozymes with phosphatidylinositol 4,5-bisphosphate, J. Biol. Chem. 266 (1991) 8727–8833.
[28] E.N. Lee, S.Y. Lee, D. Lee, J. Kim, S.R. Paik, Lipid interaction of alpha-synuclein during the metal-catalyzed oxidation in the presence of Cu2+ and H2O2, J. Neurochem. 84 (2003) 1128–1142.
[29] D.M. Jameson, J.C. Croney, P.D. Moens, Fluorescence: basic concepts, practical aspects, and some anecdotes, Methods Enzymol. 360 (2003) 1–43.
[30] P.D. Moens, M.C. Wahl, D.M. Jameson, Oligomeric state and mode of self-association of thermotoga maritima ribosomal stalk protein L12 in solution, Biochemistry 44 (2005) 3298–3305.
[31] F. Perrin, Polarisation de la Lumière de Fluorescence. Vie Moyenne des Molécules Fluorescentes. J. Phys. 7 (1926) 390–401.
[32] J. Karolin, L.B.-A. Johansson, L. Strandberg, T. Ny, Fluorescence and absorption spectroscopic properties of dipyrromethene boron difluoride (BODIPY) derivatives in liquids, lipid membranes, and proteins, J. Am. Chem. Soc. 116 (1994) 7801–7806.
[33] D.M. Jameson, E. Gratton, R.D. Hall, The measurement and analysis of heterogeneous emission by multifrequency phase and modulation spectroscopy, Appl. Spectrosc. Rev. 20 (1984) 55–105.
[34] H. Cho, Y.A. Kim, J.Y. Yoon, D. Lee, J.H. Kim, S.H. Lee, W.K. Ho, Low mobility of phosphatidylinositol 4,5-bisphosphate underlies receptor specificity of Gq-mediated ion channel regulation in atrial myocytes, Proc. Natl. Acad. Sci. U. S. A. 102 (2005) 15241–15246.
[35] F.S. Wouters, P.I. Bastiaens, K.W. Wirtz, T.M. Jovin, FRET microscopy demonstrates molecular association of non-specific lipid transfer protein (nsL-TP) with fatty acid oxidation enzymes in peroxisomes, EMBO J. 17 (1998) 7179–7189.
[36] K. Sathish, B. Padma, V. Munugalavadla, V. Bhargavi, K.V. Radhika, R. Wasia, M. Sairam, S.S. Singh, Phosphorylation of profilin regulates its interaction with actin and poly (L-proline), Cell. Signal. 16 (2004) 589–596.
[37] D.M. Jameson, S.E. Seifried, Quantification of protein–protein interactions using fluorescence polarization, Methods 19 (1999) 222–233.
[38] I. Lassing, U. Lindberg, Specific interaction between phosphatidylinositol 4,5-bisphosphate and profilactin, Nature 314 (1985) 472–474.
[39] P.A. Janmey, W. Xian, L.A. Flanagan, Controlling cytoskeleton structure by phosphoinositide–protein interactions: phosphoinositide binding protein domains and effects of lipid packing, Chem. Phys. Lipids 101 (1999) 93–107.
[40] E.K. Tuominen, J.M. Holopainen, J. Chen, G.D. Prestwich, P.R. Bachiller, P.K. Kinnunen, P.A. Janmey, Fluorescent phosphoinositide derivatives reveal specific binding of gelsolin and other actin regulatory proteins to mixed lipid bilayers, Eur. J. Biochem. 263 (1999) 85–92.
[41] P. Gascard, E. Journet, J.C. Sulpice, F. Giraud, Functional heterogeneity of polyphosphoinositides in human erythrocytes, Biochem. J. 264 (1989) 547–553.
[42] M.R. Bubb, I.C. Baines, E.D. Korn, Localization of actobindin, profilin I, profilin II, and phosphatidylinositol-4,5-bisphosphate (PIP2) in Acanthamoeba castellanii, Cell Motil. Cytoskeleton 39 (1998) 134–146.
[43] R.L. Doughman, A.J. Firestone, R.A. Anderson, Phosphatidylinositol phosphate kinases put PI4,5P(2) in its place, J. Membr. Biol. 194 (2003) 77–89.
[44] R.L. Doughman, A.J. Firestone, M.L. Wojtasiak, M.W. Bunce, R.A. Anderson, Membrane ruffling requires coordination between type Ialpha phosphatidylinositol phosphate kinase and Rac signaling, J. Biol. Chem. 278 (2003) 23036–23045.
[45] E.G. Tall, I. Spector, S.N. Pentyala, I. Bitter, M.J. Rebecchi, Dynamics of phosphatidylinositol 4,5-bisphosphate in actin-rich structures, Curr. Biol. 10 (2000) 743–746.